J. Phys. Chem. A **2002,** *106,* 8323−8327 **8323**

Measurements of Pressure-Broadening Coefficients for the $F' = 3 \leftarrow F'' = 4$ Hyperfine Line of the $^2P_{1/2} \leftarrow {}^2P_{3/2}$ Transition in Atomic Iodine[†]

S. J. Davis,* P. A. Mulhall, and M. Bachman

Physical Sciences Inc., 20 New England Business Center, Andover, Massachusetts 01810

W. J. Kessler[‡] and P. B. Keating[‡]

Confluent Photonics Corporation, 20 New England Business Center, Andover, Massachusetts 01810

Received: December 31, 2001; In Final Form: April 2, 2002

We describe a series of measurements of pressure-broadening coefficients for the $F' = 3 \leftarrow F'' = 4$ line of the $^2P_{1/2} \leftarrow {}^2P_{3/2}$ transition in atomic iodine. This is the optical transition of the chemically pumped atomic iodine laser (COIL), and our results are relevant to a more complete understanding of this important class of high-power lasers. The measurements were made in sealed cells using an argon ion laser to photodissociate molecular iodine and a tunable diode laser to probe directly the atomic transition. We measured broadening coefficients for three bath gases: He, N_2, and O_2. Full absorption line shapes were recorded as a function of the added bath gas pressure and the following values were obtained at room temperature: $(\Delta\nu/\Delta P_{He})_{T=296K} = 3.2 \pm 0.3$ MHz/Torr, $(\Delta\nu/\Delta P_{N2})_{T=296K} = 5.5 \pm 0.6$ MHz/Torr, and $(\Delta\nu/\Delta P_{O2})_{T=296K} = 5.0 \pm 0.5$ MHz/Torr; where $\Delta\nu$ is the full width at half-maximum. We also measured the temperature dependencies of the He and O_2 broadening coefficients over the range 296 K $< T <$ 775 K. We quote the temperature-dependent values as $(\Delta\nu/\Delta P_{He})_T = (3.2 \pm 0.3) \times (296/T)^{0.36}$ and $(\Delta\nu/\Delta P_{O2})_T = (5.5 \pm 0.6) \times (296/T)^{0.70}$. Comparisons to previous measurements are also discussed.

Introduction

The chemical oxygen iodine laser (COIL), demonstrated in late 1977, was the first example of an electronic transition chemical laser.[1] There has been a continuing interest in this device since that time, and there is now a rich literature concerning all aspects of COIL including: kinetics, spectroscopy, scaling, and applications. The COIL is an energy-transfer device that derives its energy from metastable, singlet molecular oxygen, $O_2(a^1\Delta)$. The oxygen is produced in the chemical reaction of chlorine and hydrogen peroxide (in a basic solution). Molecular iodine is injected into the flow, and the oxygen dissociates the I_2 into atoms which are then pumped to the $^2P_{1/2}$ state by energy-transfer collisions with the singlet oxygen. Consequently, COIL is a flowing gas device and mixing, chemistry, and heat release all play important roles in the laser performance. Indeed, heat release in the flow of early subsonic flow devices produced spatially, nonuniform population inversion profiles with a large negative gradient in the flow direction. This resulted in projections of poor beam quality for high-power COIL lasers.[2] This forced developers of higher power COILs to consider supersonic flows similar to HF laser technology.

It is widely recognized that the translational temperature in a gas flow COIL device is important from a more fundamental perspective. The detailed kinetics of COIL have been studied previously, notably by the seminal and detailed work of Heidner and co-workers,[3,4] and we present only a brief discussion. The system is described by eqs 1−3.

$$I(^2P_{3/2}) + O_2(^1\Delta) \underset{k_r}{\overset{k_f}{\rightleftarrows}} I(^2P_{1/2}) + O_2(^3\Sigma) \tag{1}$$

$$O_2(^1\Delta) + O_2(^1\Delta) \rightarrow O_2(^1\Sigma) + O_2(^3\Sigma) \tag{2}$$

$$I^* + h\nu \rightarrow I + 2h\nu \tag{3}$$

The forward reaction 1 is exothermic by 402 cm^{-1}. From statistical mechanics, the equilibrium condition for inversion of the atomic iodine in COIL is given by eq 4.

$$K_{eq} = \frac{k_f}{k_r} = 0.75\ \exp(402/T) \tag{4}$$

Consequently, at room temperature, the atomic iodine lasant species can be inverted with about 18% of the oxygen in the $a^1\Delta$ state; the fraction of the oxygen required to invert the iodine is less at lower temperatures. Any additional singlet delta oxygen can be used to derive output power from the COIL device. Since the equilibrium constant for the forward and backward rates for the energy exchange between atomic iodine and oxygen (reaction 1) is temperature-dependent, knowledge of the spatially resolved temperature profile in COIL would be valuable. Previously, we suggested that spectrally resolved absorption measurements of species within the flow field of COIL could be used to infer the temperature from the Doppler component of the line profiles.[5] Candidate species for these measurements are water vapor, molecular oxygen, and atomic iodine. We have developed sensitive monitors for each of these species on the basis of tunable diode laser absorption spectroscopy (TDLAS), and measurements of species concentration temperature have

---

[†] Part of the special issue "Donald Setser Festschrift".

* To whom correspondence should be addressed. Tel: 978-689-0003. E-mail: sdavis@psicorp.com. Fax: 978-689-3232.

[‡] Tel: 978-738-8260. Fax: 978-738-8257.

10.1021/jp014690k CCC: $22.00

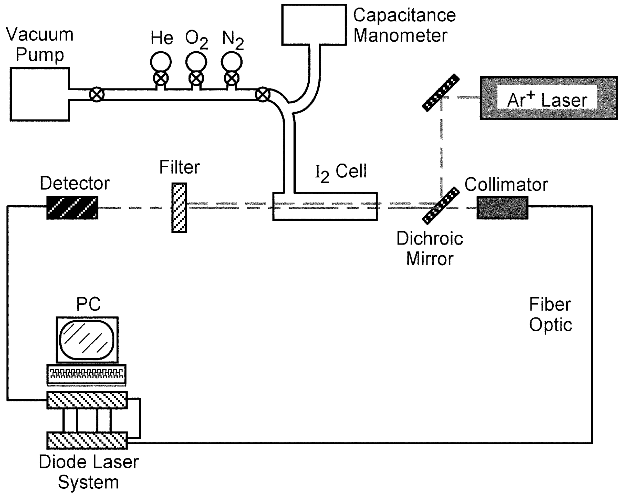

Figure 1. Apparatus used for the atomic iodine line-broadening measurements.

been reported on these species from several laboratories[6−8] using these monitors.

Accurate extraction of the Doppler (Gaussian) component of an absorption line profile requires knowledge of the collisional (pressure) broadening (Lorentzian) component. In this paper, we present the first in a series of measurements of pressure-broadening coefficients. The current paper describes measurements in atomic iodine. Subsequent papers will discuss similar measurements for the $O_2(b^1\Sigma \leftarrow X^3\Sigma)$ system and the H_2O ($\upsilon_3 + \upsilon_2$) vibrational band. All are candidates for temperature monitors in COIL, but the oxygen transition is very weak and provides less accuracy as a temperature monitor.

Pressure-broadening coefficients are important from a more fundamental perspective since they provide insight into interaction potentials between the collision partners. Consequently, there have been several prior measurements of I atom-pressure broadening. Padrick and Palmer[9] used a photolysis iodine laser to measure broadening coefficients for He and Ne at high pressures. Engleman et al.[10] completed a series of Fourier Transform Spectrometer absorption measurements at high temperatures ($T \sim 1000$ K). Neumann et al.[11] provided the first data under conditions close to COIL using a Fabry−Perot interferometer to analyze the atomic iodine emission excited by singlet oxygen. Cerney et al.[12] reported broadening coefficients obtained near room temperature by analyzing the emission from atomic iodine produced from the 496.5-nm photolysis of molecular iodine. The present measurements are the first spectrally resolved direct absorption studies at conditions relevant to COIL. We compare our results to previous measurements.

Experiment

Room-Temperature Measurements. The apparatus used for the room-temperature measurements is shown in Figure 1. Four major components comprised the apparatus: photolysis source, sample cell, diode probe laser, and data acquisition system. All experiments were performed using static cells containing molecular iodine and variable concentrations of collision partners. We used a Coherent Innova 100 argon ion laser as a photodissociation source for ground-state I atoms. We used the 496.5-nm line for the measurements reported here. Cerney and co-workers[12] also used the 496.5-nm line to produce excited state ($^2P_{1/2}$) iodine atoms, but they monitored the $^2P_{1/2} \rightarrow {}^2P_{3/2}$ emission with a Fourier Transform Spectrometer.

Previously, Tellinghuisen[13] had determined the absorption cross sections for I_2 in the visible to near-IR spectral region from the ground $X^1\Sigma$ to several excited states in molecular iodine. Burde and McFarlane[14] made similar measurements and concluded that absorption on the I_2(B−X) system could be used to produce excited, $^2P_{1/2}$ atoms. Davis[15] used these results to produce an I atom laser from dye-laser excitation of molecular iodine in the 493−499-nm region. This result, combined with Tellinghuisen's studies, indicated that the branching ratio for $I^2P_{1/2}/I^2P_{3/2}$ is about 40% for excitation at 496.5 nm. The excited atomic iodine is produced since the photon energy at 496.5 nm is above the dissociation energy of the $B^3\Pi_{0+}$ state, and it correlates to $I^2P_{3/2}$ and $I^2P_{3/2}$ at dissociation. The repulsive $^1\Pi_u$ state correlating to two ground-state atoms also strongly absorbs in this region.

The diameter of the argon ion laser photodissociation beam was approximately 4 mm in the cell. We completed all measurements using the 496.5-nm line although we confirmed production of I atoms using the 488 and 514.5-nm lines. For all measurements reported here, 650 mW of the 496.5-nm radiation was incident on the iodine cell.

The 33-cm long cell contained several, valved sidearms. One contained iodine crystals that produced the iodine vapor used in the cell. A second sidearm was connected to a gas-handling system from which the various collision partner gases could be added. A third sidearm was used to evacuate the cell before and during experimental runs. Gas-pressure measurements were made with an MKS 100 Torr Baratron capacitance manometer connected to a fourth sidearm.

We used a distributed feedback, tunable diode laser for the absorption line measurements. This device produced a single longitudinal mode output and was current tuned over the (3,4) line near 1315.2 nm. Measurements made with a Burleigh confocal Fabry−Perot spectrum analyzer indicated that the diode laser bandwidth (fwhm) was <6 MHz. The diode laser was fiber-coupled and a fiber splitter was used to produce three output legs. Each output was contained in a single-mode fiber optic. One output fiber was connected directly to an InGaAs detector/transimpedance amplifier that was used to normalize the absorption signals as the diode laser was scanned. The second fiber was connected to a collimator that produced a beam with a diameter of approximately 2 mm. This beam passed through a heated, 10-cm quartz cell that contained 200 mT of molecular iodine and was detected with an InGaAs photodiode. The heated cell was permanently sealed and was contained in a tube furnace oven. This cell was heated to 870 K to provide a steady source of atomic iodine. As the diode laser was scanned over the (3,4) absorption line, we continuously recorded this feature from the heated cell. This provided a frequency reference while the laser was scanned. It also assured that the diode laser was tuning properly.

The absolute frequency of the diode laser was determined with a Burleigh Wavemeter (WA-20). This scanning Michaelson interferometer provides the laser frequency with an accuracy of 0.02 cm^{-1}. As indicated above the diode laser output wavelength was scanned through the (3,4) hyperfine line of the atomic iodine transition by providing a ramped injection current to the diode laser. Because this process causes some heating of the diode laser, the diode laser response is often not precisely linear, and this can lead to slight nonlinearities in the diode laser scan rate as the drive current is ramped. This is a minor effect and was monitored using a Burleigh confocal resonator spectrum analyzer. The maximum deviations from a linear scan were 5% and typically were 2%. Any uncertainties in the diode laser scan rate translated directly into proportional uncertainties in the determination of the absorption line width. These uncertainties were included in our estimates of the systematic errors in our quoted results.

The third fiber optic leg also terminated in a collimator, and this output beam was launched into the 33-cm long sample cell. As illustrated in Figure 1, a dichroic mirror was used to allow the diode laser beam to be collinear with the argon laser photodissociation beam. The diode laser probe beam was 1.8 mm in diameter to ensure that it was always within the 4-mm diameter pump volume. The argon ion laser and diode laser beams were separated after passing through the cell by a 600 line/mm diffraction grating. The diode laser beam was directed onto an InGaAs detector and residual argon ion light was directed to a beam stop.

All three InGaAs detectors were connected to transimpedance amplifiers that provided stable voltage outputs directly proportional to the diode laser light incident on each respective detector. The transimpedance amplifier outputs were fed to input channels of a 1.2 MHz/s analogue to digital (A/D) data acquisition board contained in a PC. Custom software developed in a National Instruments LabWindows CVI architecture was used to record line shapes that were analyzed offline. The line shapes recorded were normalized by the reference channel (diode laser output power as a function of drive current) to account for the unavoidable increase in diode laser power as the laser was scanned in wavelength. These scans were performed by ramping the diode laser injection current at 25 Hz. Total scan widths were 3 GHz which was sufficient to capture the entire absorption line even at the highest pressures. The recorded digitized line shapes contained 900 data points which provided adequate resolution.

The procedure for an experimental determination of a line width was the same for each bath gas. The iodine sidearm was sealed and the cell was evacuated. Next, the valve connecting the cell to the vacuum pump was closed and molecular iodine vapor was admitted to the cell. A quantity of the collision partner gas was added and its pressure was measured with the capacitance manometer. We scanned the diode laser repetitively over the (3,4) absorption line. Typically, 50 scans were averaged and stored. Scans from both the sample cell and heated reference cell were stored for later analysis. This procedure was repeated for numerous added gas pressures covering the range 0−100 Torr. Pressures were changed in random order.

Measurement of Temperature Dependence of Line Broadening. The measurements described above were for room temperature since the cell was held at approximately 296 K. To determine the broadening coefficient as a function of temperature, we manufactured two Pyrex cells that were permanently sealed by a glass seal. One cell contained a small amount of iodine vapor (<100 mT) and 96 Torr of He. The second cell was identical, but contained 98 Torr of O_2 in place of the He. Each cell was 10-cm long and could be placed in a tube furnace. The sealed cells could thus be heated to known temperatures, and we could measure the broadening coefficient for a constant number density of collision partner. When combined with the pressure-dependent measurements at constant ($T = 296$ K) temperatures described above, we were able to determine the temperature dependence from $T = 296$ to 775 K. The argon ion laser was used as the dissociation source at the lower part of this temperature range. However, for temperatures above 700 K, we observed increases in the atomic iodine number density from thermal dissociation of the molecular iodine. This did not affect our measurements of the pressure broadening, however, because we always recorded the entire absorption line shape.

Analysis Of Line Shapes. We assumed a Voigt profile for the recorded line shapes. A Voigt is a convolution of a Gaussian and a Lorentzian. The absorption of the iodine $^2P_{1/2} \leftarrow {}^2P_{3/2}$ transition is given by Beer's law:

$$I_L(\nu) = I_o(\nu)e^{N\sigma(\nu_o)g(\nu)L} \tag{5}$$

where N is the number density of $I^2P_{3/2}$ at line center; $\sigma(\nu_o)$ is the absorption cross section; $g(\nu)$ is the line shape factor; and L is the absorption path length.

The line shape information is contained in the line shape factor $g(\nu)$. In general where both collisional and thermal broadening are important, $g(\nu)$ is given by the Voigt function:

$$g(\nu) = 2(\ln 2/\pi)^{1/2}\Delta\nu^{-1}{}_D\, V(y,a) \tag{6}$$

where $\Delta\nu_D$ is the Doppler width; $V(y,a)$ is the Voigt function; $a = (\ln 2)^{1/2}\Delta\nu_C/\Delta\nu_D$ is the Voigt a-factor; $y = 2(\ln 2)^{1/2}(\nu - \nu_o)/\Delta\nu_D$ is the normalized frequency, and $\Delta\nu_C$ is the collision width. The Doppler width is defined as

$$\Delta\nu_D = \nu_o/c(8kT\ln 2/m)^{1/2} \tag{7}$$

where ν_o is the absorption center frequency, c is the speed of light, k is Boltzmann's constant, T is the gas temperature, and m is the molecular weight of atomic iodine.

The collision width, $\Delta\nu_C$, is defined as

$$\Delta\nu_c = 2\sum_i \gamma_i P_i \tag{8}$$

where P is the pressure of each collision partner, γ is the collisional broadening parameter, and $\sum_i$ is the summation over all potential collision partners.

In diode laser absorption experiments, optical elements such as cell windows often produce intensity modulations in the transmitted diode laser power as the diode laser wavelength is scanned. This is usually caused by low-contrast Etalon interference fringes. For the present experiment, these were weak and the baselines of the recorded line shapes were very linear. Data reduction in these experiments consisted of fitting the observed line shape to a Voigt function using a commercial software package Peakfit (Jandel). These fits produced Voigt parameters that contained the Gaussian and Lorentzian components. Since we carefully monitored the temperature of the cell during all runs, we were able to set the Doppler width to the appropriate value, then perform the fits. We extracted the Lorentzian width that consisted of $\Delta\nu_C$ and the diode laser line width $\Delta\nu_L$. As discussed above, measurements of the laser line width with a confocal Fabry−Perot spectrum analyzer indicated $\Delta\nu_L < 6$ MHz. This value was subtracted from the total Lorentzian line width to provide $\Delta\nu_C$, the fwhm of the collisional width.

Results

Figure 2 shows the (3,4) absorption line shape and fit in the presence of 75.8 Torr of added oxygen. The residuals (difference between data and fit) were typically less than 1% for all bath gases indicating that the Voigt fit was an adequate model.

Figure 3 shows the collisional line width as a function of added oxygen. We have removed the Gaussian and diode laser line width components prior to plotting these data. Thus, the

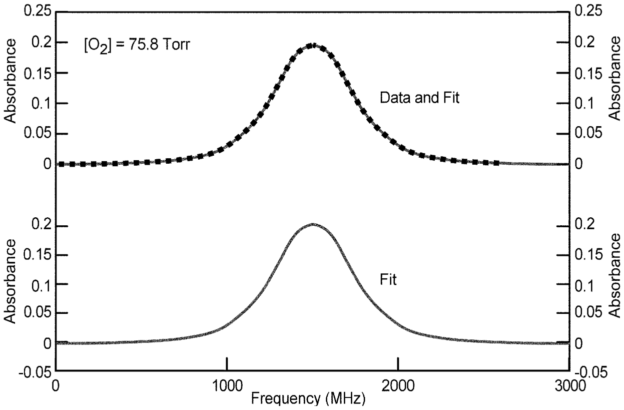

Figure 2. Atomic iodine absorption line shapes as a function of added oxygen.

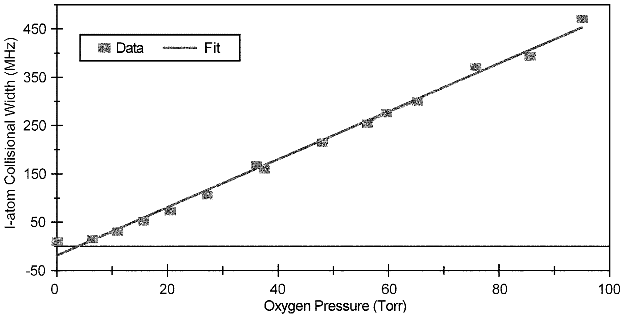

Figure 3. Collisional width of atomic iodine absorption line as a function of added oxygen.

TABLE 1: Values for Room-Temperature Broadening Coefficients and "*n*"

bath gas	broadening coefficient (2γ) at $T = 296$ K (MHz/Torr)	"n" $296 \leq T \leq 770$
He	3.6 ± 0.4	0.36 ± 0.04
O_2	5.0 ± 0.5	0.70 ± 0.07
N_2	5.5 ± 0.5	

zero bath gas intercept should be the residual line width due to broadening by molecular iodine and self-broadening due to atomic iodine. However, the number densities of these two species are both less than 0.3 Torr. Cerney et al.[12] reported a broadening coefficient by I_2 of 35 ± 10 MHz/Torr. Thus, we should expect to see an intercept about 10 MHz or less, but this is beyond the precision of our measurements. Similar data for helium and nitrogen were also obtained.

We summarize our measurements on atomic iodine at room temperature in Table 1. The uncertainties represent the standard deviations in the slopes of the respective plots of collisional widths versus pressure for the three gases studied added in quadrature with our estimate of the frequency-scanning accuracy of the diode laser.

Temperature Dependence of Broadening Coefficients. The temperature dependence of the collisional broadening coefficients for helium and oxygen were obtained from a similar analysis of the broadening of the iodine absorption line as the temperature of the two respective cells (described above) was systematically varied from room temperature to 775 K. In general, the temperature dependence of the broadening coefficient, 2γ, can be described by

$$2\gamma(T) = 2\gamma(T_0) \times (T_0/T)^n$$

where T_0 is a reference temperature, in our case room temperature (296 K), and n is a temperature-dependent parameter.[16,17]

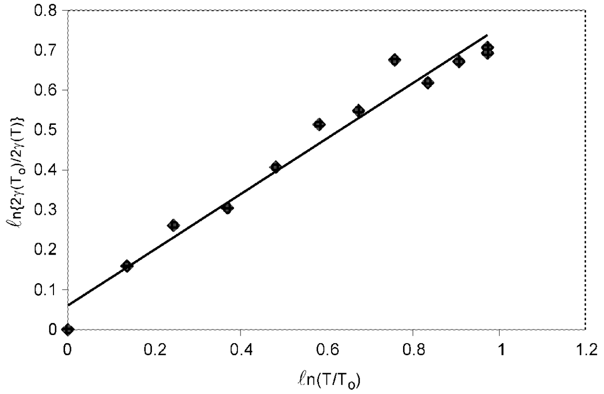

Figure 4. Plot of $\ln\{2\gamma(T_0)/2\gamma(T)\}$ versus $\ln(T/T_0)$.

TABLE 2: Comparison to Previous Results

bath gas	present results 2γ (MHz)	previous measurements 2γ (MHz)	(ref)	conditions
He	3.6 ± 0.4	3.6 ± 0.3	9	pulsed photolysis
O_2	5.0 ± 0.5	1.7	10	$T = 1000$ K (absorption)
		7.5 ± 1.5	11	$T \cong 300$ K (emission)
		4.8 ± 0.3	12	$T = 300$ K (emission)
N_2	5.5 ± 0.5	6.2 ± 0.8	9	pulsed photolysis

We can obtain an estimate for n by plotting

$$\ln\{2\gamma(T_0)/2\gamma(T)\} = n \times \ln(T/T_0)$$

Figure 4 shows a plot of this expression for oxygen broadening. Similar data were obtained for He. From these data we estimate the values of n. These values are included in Table 1.

Discussion

In Table 2, we compare our results for iodine with previous measurements. Padrick and Palmer[9] used a photolysis iodine laser to probe a gain medium containing bath gas and inferred broadening coefficients from observed changes in the peak gain on the (3,4) transition. Engleman et al.[10] used a high-resolution Fourier Transform Spectrometer (FTS) to measure broadening for oxygen, argon, and iodine at high temperatures ($T = 1000$ K). Neumann et al. [11] used a Fabry–Perot interferometer to probe the emission from atomic iodine in a flow of singlet delta oxygen and molecular iodine. More recently, Cerny et al.[12] used a Fourier Transform Spectrometer to measure collisional broadening on the atomic iodine transition relevant to COIL.

Our results are in good agreement with the previous measurements for He and N_2 at or near room temperature, that is, those of Padrick and Palmer[9] and with the O_2 results of Cerny et al.[12] However, the present results for O_2 are in rather poor agreement with the data of Neumann et al.[11] Indeed, the two results do not agree within the quoted uncertainties. The Neumann results required extensive line shape deconvolutions since the F–P interferometer had an instrumental width that was a large fraction of the actual oxygen broadened iodine line width. Thus, the Neumann et al.[11] measurements are expected to have a larger uncertainty and the disagreement with these earlier results is almost certainly due to the relatively poor resolution of the F–P spectrometer used to analyze the atomic iodine emission produced in the I_2/O_2 chemiluminescent reaction.

It is also relevant to compare the present measurements with the high-temperature results of Engleman et al.[10] Recall that they used a Fast Fourier Transform Spectrometer to analyze the absorption spectrum of atomic iodine in sealed cells at high temperature (~1000 K). They quote a broadening coefficient for O_2 of $2\gamma = 1.7$ MHz/Torr at 1000 K. Using a temperature scaling of 0.7 (see above), we would predict a room-temperature value of $2\gamma(300) = 3.6$ MHz/Torr. This is smaller than our room-temperature value and outside our uncertainty. The Engleman paper quotes no uncertainty in their measurements, so a more systematic comparison is not possible. However, a 20% uncertainty in their value at 1000 K would place their room-temperature extrapolated value within our quoted 10% uncertainty.

The temperature dependence of collisional broadening coefficients can provide insight into the interaction potential between the colliding partners. Although we have not undertaken detailed collision theory calculations, we point out that if we consider the interaction potential for He and I atom-pressure broadening to be described by a Lennard-Jones potential,[18] then one would expect that the pressure-broadening coefficient would have a $1/T^{0.3}$ dependence, consistent with our measurement of $1/T^{0.36}$.

For the oxygen case, we observe a $1/T^{0.7}$ dependence. This clearly indicates that the interaction potential is not well described by a simple Lennard-Jones model. Thus, additional terms must be considered. Several groups have developed models for collisional broadening that included higher order terms including partners with permanent electric quadrupole moments.[17,19,20] For quadrupole−quadrupole interactions, a value of $n \sim 0.75$ is commonly used.[21] Both O_2 and I have electric quadrupole moments. While we have no theoretical treatments of the temperature dependence of the $O_2 + I$ broadening, our measurements show a temperature dependence stronger than a Lennard-Jones potential and consistent with existing models. This suggests that the quadrupole−quadrupole interaction is a significant contributor to the temperature dependence of the collisional broadening.

We can also use our results to extrapolate the pressure broadening to lower temperatures. Many supersonic COIL devices operate at or near 200 K. We predict the following values for He and O_2: $\gamma_{He}(200) = 4.1$ MHz/Torr and $\gamma_{O2}(200) = 5.7$ MHz/Torr.

Acknowledgment. This work was supported in part by The Air Force Office of Scientific Research and by Physical Sciences Internal Research and Development funds. We are grateful for this support.

References and Notes

(1) McDermott, W. E.; Pchelkin, N. R.; Benard, D. J.; Bousek, R. R. *Appl. Phys. Lett* **1978**, *32*, 469.

(2) Shea, R. F. Characteristics of a supersonic oxygen iodine laser. *Laser Digest*; Technical Report AFWL-TR-80-107; Air Force Wright Laboratory: Dayton, OH, 1980; p 158.

(3) Heidner, R. F.; Gardner, C. E.; Segal, G. I.; El-Sayed, T. M. *J. Phys. Chem.* **1983**, *87*, 2348.

(4) Heidner, R. F.; Gardner, C. E.; El-Sayed, T. M.; Segal, G. I. *J. Chem. Phys.* **1981**, *74*, 5618.

(5) Allen, M. G.; Carleton, K. L.; Davis, S. J.; Kessler, W. J.; McManus, K. R. Presented at the AIAA 25th Plasmadynamics and Lasers Conference, Colorado Springs, CO, 1994.

(6) Handke, J.; Grünewald, K. M.; Duschek, F. R. Comparative studies on small signal gain and output power for COIL systems (4184−11). *Proceedings of SPIE XIII International Symposium on Gas Flow and Chemical Lasers and High-Power Laser Conference*; International Society for Optical Engineering: Bellingham, WA, 2000; pp 45−48.

(7) Rittenhouse, T. L.; Phipps, S. P.; Helms, C. A. *IEEE J. Quantum Electron.* **1999**, *35*, 857.

(8) Furman, D.; Barmashenko, B. D.; Rosenwaks, S.; Parametric studies of a small-scale chemical oxygen−iodine laser/jet generator system: recent achievements (3268−21). *Proceedings of SPIE Gas and Chemical Lasers and Intense Beam Applications*; International Society for Optical Engineering: Bellingham, WA, 1998; pp 146−156.

(9) Padrick, T. D.; Palmer, R. E. *J. Chem. Phys.* **1975**, *62*, 3350.

(10) Engleman, R.; Palmer, B. A.; Davis, S. J. *J. Opt. Soc. Am.* **1983**, *73*, 1585.

(11) Neumann, D. K.; Clark, P. K.; Shea, R. F.; Davis, S. J. *J. Chem. Phys.* **1983**, *79*, 4680.

(12) Cerny, C.; Bacis, R.; Bussery, B.; Nota, M. *J. Chem. Phys.* **1991**, *95*, 5790.

(13) Tellinghuisen, J. *J. Chem. Phys.* **1982**, *76*, 4736.

(14) Burde, D. H.; McFarlane, R. A.; Wiesenfeld, J. R. *Phys. Rev.* **1974**, *A10*, 1917.

(15) Davis, S. J. *Appl. Phys. Lett.* **1978**, *32*, 656.

(16) Tsao, C. J.; Curnutte, B. *JQRST* **1962**, *2*, 41.

(17) Bonamy, J.; Robert, D.; Boulet, C. *JQRST* **1984**, *31*, 23.

(18) Corney, A. *Atomic and Laser Spectroscopy*. Oxford Press: New York, 1986.

(19) Delaye, C.; Hartmann, J.-M.; Taine, J. *Appl. Opt.* **1989**, *28*, 5080.

(20) Labani, B.; Bonamy, J.; Robert, D.; Hartman, J.-M.; Taine, J. *J. Chem Phys.* **1986**, *84*, 4256.

(21) Lowry, H. S., III.; Fisher, C. J. *JQRST* **1984**, *31*, 575.